

## Spatio-temporal variability of NDVI–precipitation over southernmost South America: possible linkages between climate signals and epidemics

This article has been downloaded from IOPscience. Please scroll down to see the full text article.

2008 Environ. Res. Lett. 3 044008

(<http://iopscience.iop.org/1748-9326/3/4/044008>)

View [the table of contents for this issue](#), or go to the [journal homepage](#) for more

Download details:

IP Address: 200.70.57.126

The article was downloaded on 14/09/2011 at 16:25

Please note that [terms and conditions apply](#).

# Spatio-temporal variability of NDVI–precipitation over southernmost South America: possible linkages between climate signals and epidemics

Y M Toure<sup>1,2</sup>, L Jarlan<sup>3</sup>, J-P Lacaux<sup>4</sup>, C H Rotela<sup>5</sup> and M Lafaye<sup>6</sup>

<sup>1</sup> METEO-France, Meteopole, 42 Avenue Coriolis, 31057 Toulouse Cedex 1, France

<sup>2</sup> Lamont Doherty Earth Observatory (LDEO), Columbia University, Palisades, NY 10964, USA

<sup>3</sup> Centre d'Etudes Spatiales de la Biosphère (CESBIO), 18 avenue Edouard Belin, F-31401 Toulouse Cedex 4, France

<sup>4</sup> Université Paul Sabatier (UPS), Observatoire Midi Pyrénées (OMP), 12 Avenue Edouard Belin, 31400 Toulouse, France

<sup>5</sup> Instituto de Altos Estudios Espaciales 'Mario Gulich', Comisión Nacional de Actividades Espaciales (CONAE), Universidad Nacional de Córdoba, Argentina

<sup>6</sup> CNES, DSP/ARP/AV, 18 Avenue Edouard Belin, F-31401 Toulouse Cedex 4, France

Received 3 June 2008

Accepted for publication 1 December 2008

Published 15 December 2008

Online at [stacks.iop.org/ERL/3/044008](http://stacks.iop.org/ERL/3/044008)

## Abstract

Climate–environment variability affects the rates of incidence of vector-borne and zoonotic diseases and is possibly associated with epidemics outbreaks. Over southernmost South America the joint spatio-temporal evolution of climate–environment is analyzed for the 1982–2004 period. Detailed mapping of normalized difference vegetation index (NDVI) and rainfall variability are then compared to zones with preliminary epidemiological reports. A significant quasi-biennial signal (2.2- to 2.4-year periods, or QB) for joint NDVI–rainfall variability is revealed. From rotated EOFs, dominant NDVI patterns are partitioned according to their lead frequencies: (1) the 'QB group' (2.1- to 3-year periods) includes six modes over southern Brazil, Uruguay, northern-central Argentina (two modes), the southern Paraguay–northern Argentina border, and the Santa Cruz Province; (2) the QB1 (2.4- to 3-year periods) + quasi-quadrennial (QQ) mode over the Misiones Province; and (3) the QB2 (2.1- to 2.5-year periods) + QQ + inter-annual (IA) (3- to 7-year periods) two modes over south-eastern Argentina. Modes within the 'QB group' are positively correlated with global climate signals and SST. The Uruguayan mode is correlated with global ENSO (8-month lag) whilst the southern Entre-Rios/northern Buenos Aires provinces are correlated with central equatorial Pacific SSTs (3-month lag). The Santa Cruz (Patagonia) Province is most correlated with the Pacific South America (PSA) index and SST patterns (3-month lag) along the Antarctica circumpolar current. The spatial distribution of lead NDVI modes includes the Formosa, Misiones, Chaco and Buenos Aires provinces among others, known for being prone to vector-borne epidemics such as dengue fever, malaria, leishmaniasis (American cutaneous leishmaniasis or ACL), hantavirus, chagas and Argentine hemorrhagic fever (AHF). Some provinces also correspond to regions where lead NDVI PCs' modes are associated with high-frequency climate signals such as the quasi-biennial oscillation in northwest Argentina. The joint preliminary results (climate–environment–public health reports) presented here for the first time are meant: (1) to contribute to a better understanding of climate–environment–epidemics process-based and modeling studies and (2) to facilitate, in the long run, the implementation of local and regional health early warning systems (HEWS) over southernmost South America. The latter is becoming crucial with ever-increasing migration, urban sprawl (re-emergence of dengue fever epidemics since the late 1990s), all embedded in a climate change context.

**Keywords:** climate and environment, NDVI, epidemics, southernmost South America

## 1. Introduction

The spatio-temporal variability of precipitation and temperature modulate vegetation phenology, with feedback onto the lower-troposphere. Regional ecosystems' dynamics are directly affected by water and energy exchanges through the ground–vegetation–atmosphere interfaces (Van den Hurk *et al* 2003). The normalized difference vegetation index (NDVI) can thus be used as a good proxy for evaluating regional and local climate variability/changes and potential linkages with variability in regional ecosystems and local ecotones. South America is one of the continents most affected by changes in the general circulation (Minetti and Sierra 1989) and climate events such as global ENSO. During Pacific El Niño (La Niña) years, precipitation in south-eastern South America has been found above (below) normal (Ropelewski and Halpert 1987). By 'trophic cascading effects', crop yields (relying strongly upon rain-fed agriculture), public health and socio-economical issues in South American countries are found to be strongly impacted (Podesta *et al* 1999, Poveda *et al* 2001).

The NDVI has been defined and analyzed first by Tucker (1979) using National Oceanic and Atmospheric Administration (NOAA) Advanced Very High Resolution Radiometer (AVHRR) data. Later on, Los *et al* (2001) studied the co-variability between NDVI, precipitation, temperature and sea surface temperature (SST) on global scales, for about a decade. In the meantime, Myneni *et al* (1996) showed that positive NDVI anomalies over south-eastern America were linked to tropical Pacific SST warming. Finally, del Rosario Prieto (2007) highlighted linkages between ENSO events and Paraná River floods during colonial times, whilst Barbosa *et al* (2006) found that vegetation patterns in north-eastern Brazil reflected impacts from enhanced aridity during the last decade of the 20th century, and Paruelo *et al* (2004) have proposed linkages between NDVI trends over South America and climate change since 1981.

The main objective of this study is to isolate areas (pattern-based statistical approach) and lead frequencies of NDVI variability over southernmost South America. This is accomplished by using the most recent and calibrated datasets (see section 2) with large spatio-temporal extents from remote sensing. It is then to extract the joint spatio-temporal variability of NDVI–precipitation. Possible linkages with climate signals and global SST patterns and indices for the 1982–2004 period are discussed. Climate conditions (variability and change) can impinge on human health through different pathways (see figure 2 in the ESSP GEC report, 2004). It is recognized that other non-climatic factors might also be involved with public health issues, i.e. changes in irrigation techniques and agricultural practices, deforestation and urbanization, among others. At this time, there is little understanding of disease ecology in each instance (needed to make predictions) whilst the current understanding of processes and mechanisms involved is incomplete.

In a climate and environment changes' context, modulation of natural climate signals and variability, and increased demographic processes, epidemics are re-emerging worldwide (i.e. new cases of St Louis encephalitis were reported in the

Cordoba Province in 2005, Diaz *et al* 2006; new cases of previously eradicated yellow fever since the late 1950s were recently declared in the Misiones Province of Argentina in 2008). It is hoped that by working with trans-disciplinary Argentinean experts (i.e. teledetectors, entomologists, virologists, etc) through the joint French and Argentinean Spatial Agencies (CNES and CONAE) MATE (Monitoreo Argentino para Tele Epidemiologica) Project, the understanding of epidemics' outbreaks and mechanisms will be improved. This is particularly true for diseases such as dengue fever, Argentine hemorrhagic fever (AHF), malaria, leishmaniasis, hantavirus, chagas and hydatidosis, in prone regions such as the Formosa, Salta and Jujuy provinces (northwest Argentina), the Bolivian–Paraguay borders, the Entre-Ríos–Corrientes–Misiones and Chaco provinces, Patagonia region and the Argentinean–Brazilian border (Gorla 2002, Yates *et al* 2002, Avilés *et al* 2003, Guerra *et al* 2006, EID Updates 2008).

## 2. Data and methods

The studied area is the southernmost 'South America window' (22°S–52°S and 75°W–52°W), chosen to exclude equatorial and tropical areas where NDVI can be 'saturated' from high leaf area index (LAI) and potentially 'contaminated' by cloud deep convection. The Andes Mountains in the western part of the window are masked for obvious reason. The 'window' includes data from parts of Paraguay, Uruguay, southern Brazil and southern Bolivia, and the whole of Argentina. Overall the land cover is, in general, composed of C3 grasses in the southernmost part of the 'window' and along the lee-side of the Andes Mountains. Over Argentina, C4 grasses dominate over nearly all the northern half with some sparse C4 crops (following Masson *et al* 2003). Deciduous and evergreen trees are present over Uruguay and southern Brazil. The 'window' is both influenced by tropical atmospheric circulation to the north, and by seasonal rainfall events and perturbation to the south during austral winter.

The NDVI takes advantage of different spectral responses from chlorophyll-loaded vegetal tissues when using red and infrared channels (values range from 0.1 to 0.8 for vegetated areas). The latest NDVI dataset used here is from the Global Inventory Modeling and Mapping Studies (GIMMS) team, or NDVIg, for a 25-year period: 1982–2006. The data is derived from NOAA/AVHRR imagery using the NOAA satellite series 7, 9, 11, 14 and 16. New features from this upgraded dataset include reduced unwanted NDVI variations arising from calibration procedures, varying viewing angles, influence of volcanic aerosols and other effects not related to actual changes in vegetation cover. For example, data from NOAA-9 descending node had volcanic stratospheric aerosols' corrections during 1982–1984 and 1991–1994. NDVI has also been improved using the empirical mode decomposition/reconstruction (EMD) technique to minimize side effects from orbital drifts. Recent studies have shown good results from minimizing the above effects (Kaufmann *et al* 2000, Lotsch *et al* 2003, Slayback *et al* 2003). The original NDVIg dataset is submitted to maximum value compositing procedures on a 15-day basis, with an 8 km spatial resolution

(Tucker *et al* 2005). Here the spatio-temporal resolutions are up-scaled to a 0.5° grid-point system with one value per month. Prior to the analyses, the monthly NDVI data is standardized, with linear trends removed using the least-squares method.

A precipitation dataset (GPCC) is available from the Deutscher Wetterdienst (DWD, National Meteorological Service of Germany). The gridded-field on a 0.5° × 0.5° latitude longitude resolution can be obtained at <http://gpcc.dwd.de>. The ‘full data re-analysis products’ (FDRP), used here, include rainfall data from all available stations, with near-real-time and delayed observing modes (FDRP version 3 is for the 1951–2004 period).

The datasets described above are analyzed jointly using the multi-taper method/singular value decomposition (MTM/SVD) to highlight the first joint temporal coherence of NDVI and rainfall variability during the overlapping 1982–2004 period. The multivariate frequency-domain decomposition technique has been successfully developed by Mann and Park (1994). The MTM/SVD technique seeks to retain shared statistical information from the NDVI and precipitation datasets, in terms of maximum variance found for narrow-frequency bands at a given location. Thus a so-called local fractional variance, or LFV spectrum, can be plotted as a function of frequencies while significance levels are obtained from 1000 Monte Carlo simulations (Mann and Park 1996). The code can be obtained at: <http://www.people.virginia.edu/~mem6u/mtmsvd.html>.

The NDVI data alone is also submitted to rotated empirical orthogonal function (EOF) analyses using the Varimax criterion (Richman 1986) to identify key regions of variability. The rotation eliminates potential eigenvalue degenerescence (overlapping) from sampling errors (North *et al* 1982) and allows for identification of potential simple spatial structures. Twenty-five EOF ranked modes are retained prior to rotation, still representing ~80% of total variance but for a simplified dataset. Thus, regions where significant NDVI signals are spatially coherent can be plotted within the studied window.

MTM spectra are obtained for the first 10 rotated principal components (PCs) obtained above. Three ‘filters’ are used for reasonable frequency resolution, which still provide sufficient degrees of freedom for adequate signal/noise decomposition (Mann and Park 1994). Peaks from the spectra are associated with periodic signals, and their significance levels are relative to an estimated ‘red-noise’ background. This null hypothesis is motivated for dynamical reasons when studying geophysical phenomena. Resulting significant climate signals associated with vegetation cover variability, combined with results from the joint NDVI–precipitation MTM/SVD analyses, are compared with epidemiological datasets.

Based upon direct regional reports from the Dirección de Epidemiología, Ministerio de Salud, Argentina, and results from lead epidemiological scientific papers, the geographic distribution for key endemo-epidemics was produced in figure 5 and compared with the location of the centers of the NDVI modes obtained from the rotated EOFs analysis (figure 2, bottom) for easier interpretation.

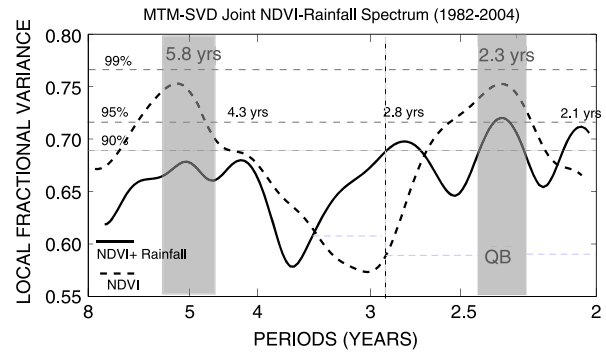


**Figure 1.** Joint NDVI–rainfall local fractional variance (LFV, on ordinate axis) for the 1982–2004 period (solid line). NDVI LFV is given for comparison (dashed line). The significance levels from boot-strapping are obtained from the three horizontal dashed lines (90%, 95% and 99%). Peak frequencies from polynomial smoothed spectra are given. QB is for quasi-biennial band (shaded). Periods (years) are given on the abscissa.

### 3. Results

In figure 1, individual NDVI and joint NDVI–rainfall LFV are displayed for the 1982–2004 period. It can be seen that a joint QB signal (gray-shaded area to the right) with a 2.3-year peak (after polynomial smoothing) is significant at the 95% level. The other three peaks (i.e. 2.1- 2.8- and 4.3-year periods) reflect power spectra for the LFV rainfall alone (not shown). A 5.8-year period is found (gray-shaded area to the left) but below the 90% level due to the relative shortness of the time series (it is highly significant though for the LFV of NDVI alone, represented by the dashed line). When the evolutive spectrum is examined with an 8-year moving window (not shown) it is found that the significant QB band is present during most of the period under investigation (with LFV values smaller than 0.72, the 95% level, prior to 1989 and between 1992 and 1995).

In figure 2, spatial distribution of explained variance (from 40% up to 80%, shaded red) from the nine out of the first ten rotated and ranked EOF modes (which represent ~42% cumulated total variance) are partitioned based upon their dominant frequencies in their MTM PCs spectra (figure 2, top). Interestingly enough the sorted patterns correspond to specific bio-climatic domains: the first panel or ‘QB group’ (figure 2, bottom left) with rotated EOF modes 1, 2, 3, 10, 8 and 6 includes southern Brazil, Uruguay and central, northern and the extreme south of Argentina. Mode 4 over the Salta Province is not shown since it displays a maximum explained variance of 60%. The seasonal rainfall distribution for the first panel is slightly bi-modal with no real dry season. It is essentially covered by Sertão’s vegetation types (Rio Grande do Sul, mode 1), fertile coastal lowlands and grasslands (mode 2), complex ecosystems of marshes, ponds, lagoons and wetlands (mode 3), and rice, soja, wheat cornfields and orchards (mode 10). Mode 8 covers the Formosa Province (east of the Salta Province) on the southern border of Paraguay, with a subtropical climate (~1000 mm/year of rain), a jungle-type forest and the ‘impenetrable’ region to the west with the typical Chaco forest. Dengue and chagas epidemics are prevalent there



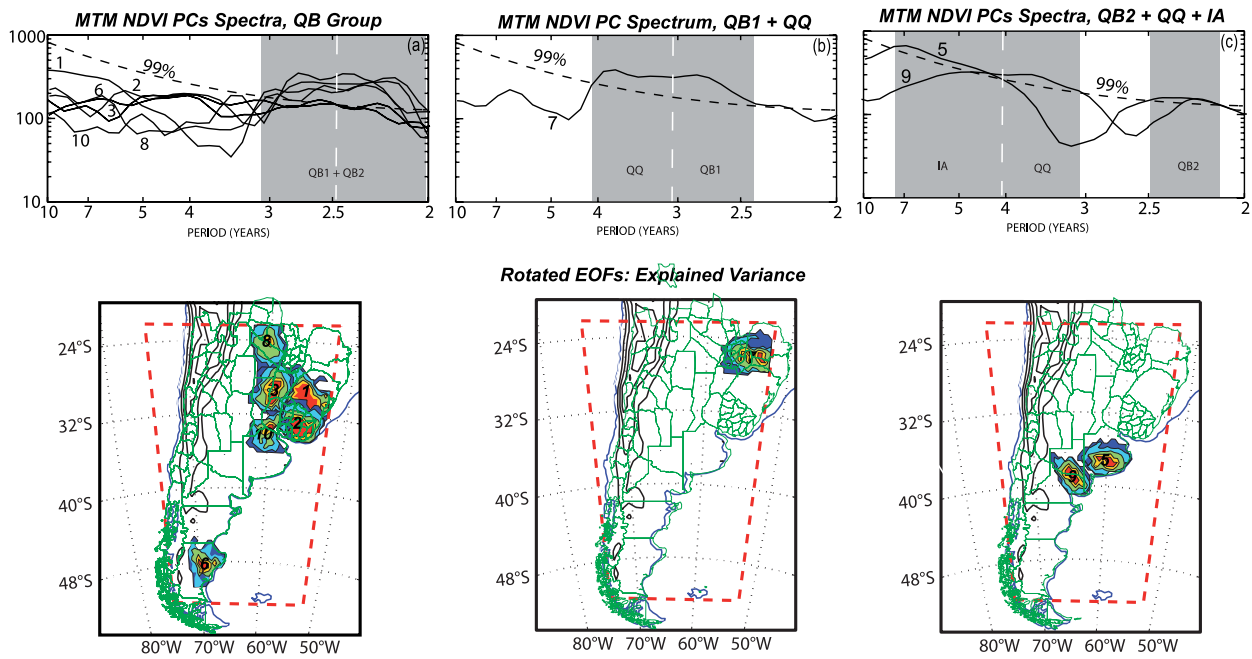


**Figure 2.** (Top) MTM PCs’ spectra from the NDVI rotated EOFs using NOAA/AVHRR GMMS (NDVI<sub>g</sub>) dataset during the 1982–2004 period. Dotted lines correspond to the 99% confidence level (red-noise hypothesis). On the ordinates standardized units ( $\times 100$ ) are given. Significant QB bands are found for the three panels: panel 1, top left; panel 2, top middle and panel 3, top right. Significant QQ and Inter-annual signals are also found in panels 2 and 3. Periods (years) are given on the bottom axis. (Bottom) Explained variance of corresponding rotated EOFs modes over the southern ‘South America window’ (21°S; 52°S and 75°W; 52°W, red dashed line). Three spatio-temporal regions/panels have been isolated: (a) panel 1 (bottom left) with six rotated EOF modes, (b) panel 2 (bottom middle) with one isolated rotated EOF mode and (c) panel 3 (bottom right) with two rotated EOF modes. Colors represent the percentage of explained variance for each mode, starting at 40% (blue) to 80% (red), using 10% incremental steps. QB is for quasi-biennial, QQ is for quasi-quadrennial and IA is for inter-annual. The Andes (black contour) are masked for the analysis.

(Diosque *et al* 2004). On its western side is a fertile valley with cardón cacti on the outskirts and tropical highland forests. To its extreme northwest on the lee-side of the Andes, the climate is very hot during summers (up to 40 °C) while cold winters dominate. The towns of Orán (Salta Province), Resistencia (Chacos Province) and Corrientes (Corrientes Province) and neighboring areas are densely populated and dengue fever epidemics re-emerge; the isolated mode 6, to the extreme south, is found over the Santa Cruz Province–Patagonia area where hydatidosis is present. The latter region is covered by shrub steppes (extreme southern part of the ‘window’) and is under the influence of both the Pacific and Atlantic Oceans with rainfall amounts less than 200 mm/year. The second panel includes only one rotated EOF mode (figure 2, bottom middle) which covers mostly the north of the Corrientes Province and the Misiones Province (mode 7). This is a region where dengue, malaria and leishmaniasis epidemics are also re-emerging. The third panel includes two rotated EOF modes (figure 2, bottom right) covering most of the Buenos Aires (mode 5) and the southern Buenos Aires–La Pampa–Rio Negro (mode 9) provinces with  $\sim 500$  mm/year rainfall. Grass, sorghum, corn, sunflower and a few ombú or algarrobo trees dominate there. In the Pampa, flooding can be severe and Argentina hemorrhagic fever (AHF) is endemic (Polop *et al* 2008) within a humid environment. Cases of hantavirus (Porcasi *et al* 2005) and hydatidosis (Lamberti *et al* 1999) have also been recorded there.

The MTM PCs spectra which allowed for associating modes into three panels, based upon lead frequencies, are displayed in figure 2 (top left for ‘QB group’; top middle for single mode 7; top right for panel 3). Significant variances (99% confidence level) are found within two frequency bands: a wide QB band (2.0- to 3.1-year periods which includes QB1 or 2.4- to 3.1-year periods and QB2 or 2.2- to 2.5-year periods) only for the ‘QB group’; a wide QB1 (2.4- to 3.1-year periods) plus QQ (3.1- to 4.1-year periods) band for isolated mode 7; a narrower QB2 (2.2- to 2.5-year periods) band, and a wide QQ and IA (3.1- to 7.1-year periods) bands for panel 3, with peaks at  $\sim 3.7$ -year (QQ) and  $\sim 6.8$ -year (IA) periods.

Further insight into possible linkages with associated climate signals is gained by correlating the NDVI PC modes to SST indices such as: ‘NINO3’ in the equatorial Pacific Ocean (150°W–90°W and 3°S–3°N, from OGP/NOAA), ‘ATL3’ in the equatorial Atlantic Ocean (20°W–GMT and 3°S–3°N, following Servain 1991), and the PSA 500 hPa geopotential index as defined by Mo (2000), and re-analyzed by Robertson and Mechoso (2003). Modes 1, 2, 3 and 10 from the QB group are all significantly correlated with NINO3:  $r = 0.52, 0.71, 0.62$  and  $0.50$  at  $\sim$  half-a-year lags, while mode 6 (Santa Cruz Province) is correlated with PSA:  $r = 0.57$  at 0 lag. Mode 7 from panel 2 is correlated with NINO3 ( $r = 0.64$  at half-a-year lag). Mode 9 from panel 3 is anti-correlated with ATL3:  $r = 0.56$  at 5-month lag.

Lead/lag correlations between all NDVI PCs and global SST are computed and mapped. The most significant

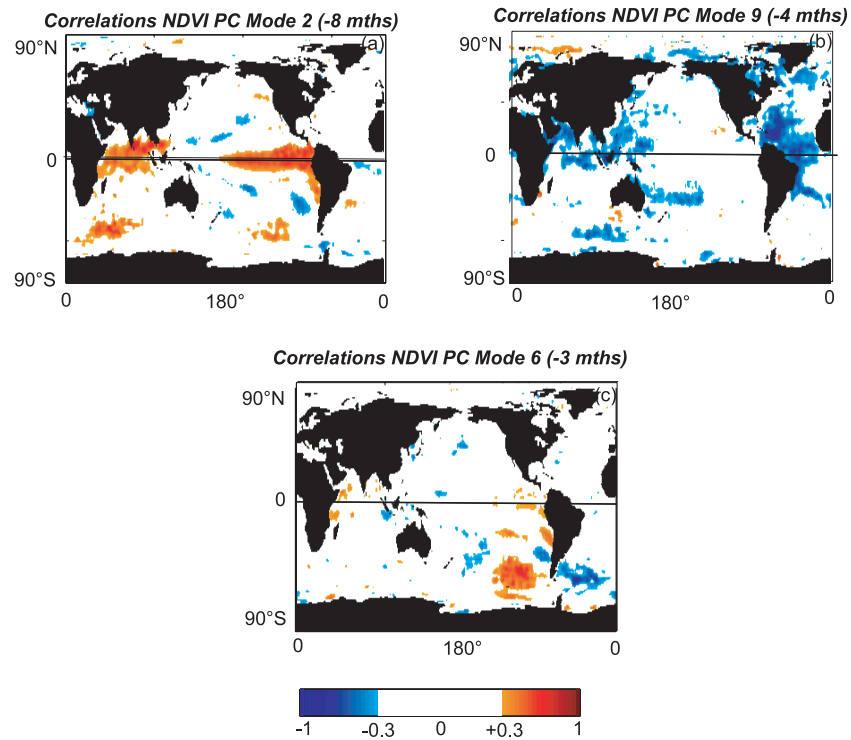


**Figure 3.** Examples of significant correlations between global SST and rainfall obtained from three different NDVI modes, i.e. mode 2 (Uruguay, ‘QB group’), mode 9 (La Pampa–Rio Negro provinces, from panel 3) and mode 6 (Santa Cruz Province, ‘QB group’). Correlations are given in the colored scale at the bottom.

and homogeneous patterns are presented in figure 3, i.e. correlations between PCs from mode 2 (Uruguay, QB group; figure 3, top left), mode 9 (La Pampa–Rio Negro provinces, panel 3; figure 3, top right) and mode 6 (Santa Cruz Province, the mode to the extreme south from the ‘QB group’, figure 3, bottom). The global ENSO signature is recognized in figure 3 (top, left) with equatorial Indian Ocean warming, central and eastern tropical Pacific warming, west equatorial Atlantic cooling and two warming cores in the Antarctica circumpolar current (ACC, maximum correlations at 8-month lag). The patterns associated with mode 10 (northern Buenos Aires, Entre-Rios Province between Rios Paraná and the Uruguay river, southern Santa Fe Province) correspond to central equatorial Pacific warming (not shown), such as during the early stages of the 1982–83 El Niño event. Linkages between NDVI PC over the southern Buenos Aires–La Pampa–Rio Negro provinces (mode 9) with western tropical Atlantic SST are recognized from patterns displayed in figure 3 (top right), with maximum correlations at 4-month lag. The specific SST patterns of the ACC in the vicinity of the South American tip are noticed in the NDVI PC over Santa Cruz (mode 6) with maximum correlations at 3-month lag (figure 3, bottom). Global SST patterns with rainfall amount over key NDVI regions and possible relationships with areas with epidemics outbreaks of a few diseases are discussed next.

#### 4. Discussion and conclusion

Using the latest and best available datasets, linkages between NDVI dominant patterns of variability over regions of

southernmost South America, local rainfall amount and dominant climate signals from neighboring oceans have been highlighted for the first time. For the relatively short period under investigation, the influence of ENSO with its different spatio-temporal scales on NDVI and rainfall variability are seen. Overall it is characterized by the wide ‘quasi-biennial’ (QB) and inter-annual/quasi-quadrennial (IA/QQ) bands, all belonging to the ENSO spectrum and distinct SST spatial patterns in the Pacific Ocean (Tourre and White 2005). The wide QB band includes two quasi-biennial sub-bands QB2 and QB1 with spectral peaks centered around periods of 2.3 and 2.7 years, as in Tourre *et al* (1999) and Tourre and White (2006). Early on, Angell and Korshover (1974) argued that the QB fluctuations with different frequencies are linked to the southwest–northeast movement of the so-called ‘centers of action’. Later, QB signals were identified in SLP anomalies over the Northern Hemisphere (Trenberth and Shin 1984) and from global analysis of air temperature and SST (Mann and Park 1994).

For the 1982–2004 period, the significant (95% level) joint NDVI–rainfall frequency variability is within a narrow QB band with a 2.3-year peak, as in the global QB climate signal (White and Allan 2001). Findings here corroborate results from Los *et al* (2001) but for a shorter period, when they identified a strong global NDVI signature near a 2.6-year period. Tourre *et al* (1999) and Tseng and Mechoso (2001) also observed the two significant QB climate signals in the Atlantic Ocean, while Jarlan *et al* (2005) isolated a QB NDVI signal over west Africa, among others. The presence of the QB signal in the La Pampa Province is in agreement with results

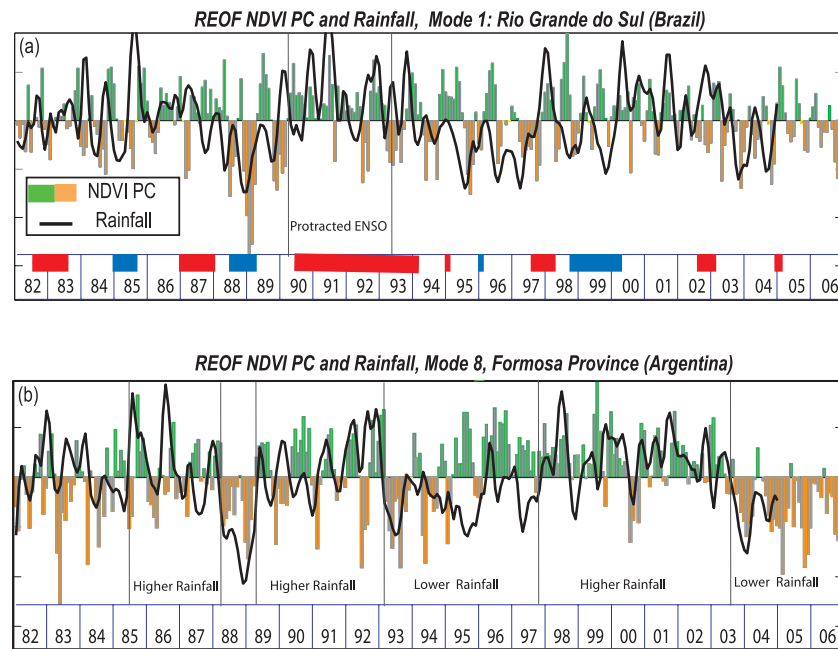


**Figure 4.** Examples of complex temporal linkages between rainfall (solid black line) and NDVI PCs (green and brown bars): (1) ENSO (including QB and protracted ENSO) influences in the Rio Grande do Sul of Brazil (top) and (2) low-frequency climate modulation on NDVI and rainfall variability in the Formosa Province of Argentina (bottom). Standardized units are on ordinates.

by Kestin *et al* (1998). They also documented an increase in the amplitude of the QB signal at the end of the 20th century, probably due to climate change. It is interesting to note that, during the investigated period, the other key individual NDVI signal with a peak at 5.8 years is present and could correspond to another ENSO timescale, as in Tourre and White (2005).

Out of the 10 leading NDVI rotated EOF modes, significant QB signals (QB1 and QB2) are also present in nine modes (6 modes in the so-called ‘QB group’, including an isolated mode in the extreme south of Argentina or the Santa Cruz Province–Patagonia), 1 isolated mode in panel 2 with the ‘lower-frequency’ QB1 and QQ signals and 2 modes in panel 3, with the ‘higher-frequency’ QB2 and IA/QQ signals. The latter panel includes the Rio Grande do Sul region in Brazil and the Misiones Province of Argentina. The inter-annual (IA) variability of vegetation conditions there is noticeable and makes that region different from the ‘QB group’. For instance, over La Pampa positive NDVI anomalies are found when positive rainfall anomalies occur during El Niño events from November to January (not shown), thus corroborating findings by Pisciotano *et al* (1994). The opposite holds true during La Niña events, with NDVI negative anomalies during springtime as in Grimm *et al* (1998). An Atlantic 4.4-year signal is being linked to local equatorial Atlantic–Ocean–atmosphere interactions. The prominent QQ signal from panel 2, located in the subtropical regions and present over the Misiones Province (~24–30°S), is coherent with results from Ribera and Mann (2003). Finally, the QB and IA/QQ bands found in all three panels belong to the extended ENSO spectrum as in Tourre and White (2006).

Significant positive lagged correlations (at the 99% confidence level) between NINO3 and several NDVI modes from the QB group means that an ocean warming over the

NINO3 box leads to enhanced rainfall (and NDVI increase) over the considered region. This is corroborated by the correlation maps between NDVI PCs and global SST spatial patterns. The negative correlation between NDVI in mode 9 (La Pampa) on the Atlantic side with western tropical Atlantic SST with ~3-month lag might be due to the transmission of the QQ ENSO signal from the Pacific into the Atlantic, with contemporaneously changes in the thermal state of the southern Atlantic, as identified by Tourre and White (2005). Moreover, positive lagged correlations between NDVI mode 6 (Santa Cruz–Patagonia) and PSA (the southern hemisphere equivalent of the PNA pattern in the northern hemisphere) corroborates results obtained by combining rainfall analysis and patterns, and the PSA index (Mo and Paegle 2001): the positive phase of PSA is associated with positive rainfall anomalies over the whole southern South America region during December–January–February. Over Patagonia the significant QB fluctuation could be associated with the phasing of the southern hemisphere annual mode and shifts of the circumpolar trough as modeled by Garric *et al* (2003). Finally, the significant correlation with global SST at the tip of South America could be as well associated with the variability of the Antarctic circumpolar wave as identified by White and Petersen (1996) and White (2004).

The complex relationships between NDVI, precipitation, land cover types, local hydrology and multi-scale climate variability can be further investigated by computing actual rainfall anomalous time series averaged at grid points from all the significant NDVI modes and compared with corresponding NDVI PCs. As an example, two areas, both from the ‘QB group’ with distinct temporal features, are displayed in figure 4: the Rio Grande do Sul region (mode 1, figure 4 top) and the Formosa Argentinean Province (mode 8, figure 4

bottom). In figure 4 (top), besides strong QB rainfall and NDVI variability as expected, the relationship between ENSO events (time of occurrence given on the abscissa), rainfall amount and NDVI anomalies are conspicuous, i.e. contemporaneously such as during the two large 1982–83 and 1997–98 ENSO events or during 1990–1994 when a protracted ENSO occurred (Weisberg and Wang 1997), or possibly linked to low-frequency climate variability in the South Atlantic (Venegas *et al* 1996), or slightly lagged like in 1985 or 2002. In figure 4 (bottom), in the Formosa Province, while a QB signal again dominates the NDVI PC (see figure 1, top left) there is evidence (not statistically significant due to the shortness of the records) of low-frequency (Tourre and White 2006) and in-phase NDVI–rainfall variability. The latter is particularly true between 1986 and 1992, and after 1996 onward. For mode 7 (Corrientes and Misiones Provinces) a unique QQ NDVI signal dominates the PC and transient in-phase relationships between NDVI and rainfall anomalies can be found on these timescales (like from 1988 to 1991, not shown).

Climate variability is only one component associated with epidemics outbreaks (i.e. new, existing with some periodicity and/or re-emerging). Ecosystem responses to climate variability can be seen as ‘mediators’ on diffusion of infectious vector-borne and rodent-borne diseases (following Root *et al* 2003). Woodland savannas, tropical forests and ecotones are indeed areas with plant and animal biodiversity with complex distribution (Patz *et al* 2004) and variability. Rain-fed agriculture highly dependent on climate variability is also directly linked to public health (Trewavas 2002). Results presented here on climate–environment variability are meant to contribute first to a better understanding of mechanisms possibly linked with outbreaks and diffusion of diseases and distribution of pathogens’ reservoirs. The distribution of reported disease cases in the studied ‘window’ can be found in figure 5. The centers of lead NDVI modes are given to compare easily with disease-prone areas. It is interesting to note that Argentine hemorrhagic fever (AHF), as identified by Polop *et al* (2008), prevails where the NDVI modes 10 and 5 are found. Mode 10 is also in a zone where hantavirus dominates and can include preferred areas for rodents’ habitats and reservoirs of zoonoses (Sergio Sosa-Estani *et al* 2001, Porcasi *et al* 2005). Mode 1 which belongs to the QB group (essentially the State of Rio Grande do Sul, Brazil) encompasses a region where leishmania (*Viannia*) is encountered (Fagundes *et al* 2007) and deserves further investigation for possible physical mechanisms involved. American Cutaneous Leishmaniasis (ACL, Córdoba-Lanúsa *et al* 2006), dengue fever occurrences and malaria epidemics events have been recorded where modes 8 (Formosa Province) and 7 (Misiones Province) display strong QB and QQ variability. Hydatidosis cases are reported over La Pampa–Rio Negro provinces (Lamberti *et al* 1999), a region covered by mode 10. All of the above remarks warrant further statistical and quantitative investigations on the role climate–environment variability can play in terms of spatio-temporal appearance and diffusion of diseases.

It is acknowledged that epidemics such as dengue fever and malaria in northern Argentina (Salta, Formosa and Misiones provinces, among others) are also emerging

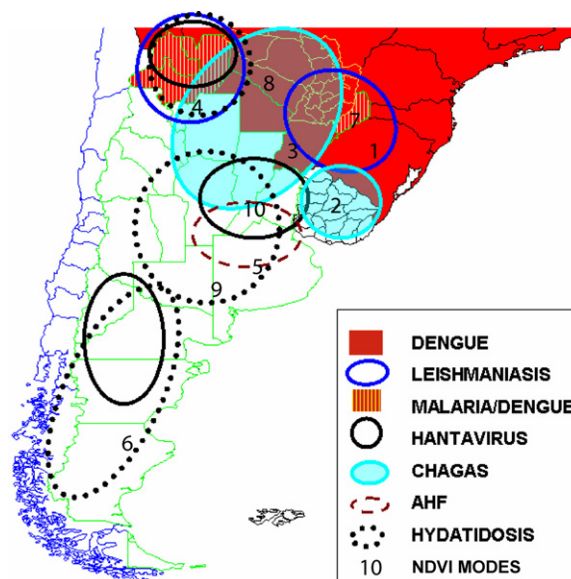


**Figure 5.** Mapping of key endemic and endemo-epidemic zones in the southernmost South America (except Chile). The geographic distribution is to be compared to those of NDVI modes, highlighted in figure 2 (bottom) and whose centers are given here. The center for NDVI mode 4 is also given with a maximum explained variance of 60%.

where urban sprawl, intense mobility of population through neighboring countries and climate change become congruous processes. For example, new and early detection of circulation of dengue fever virus have occurred only since 1997 (Avilés *et al* 2003). Malaria is re-emerging in rural areas of Jujuy and Salta provinces (along the Bolivian border) and the Corrientes and Misiones provinces (along the Paraguayan border). Nevertheless it has been recently observed (since 1998 onward, data from the Dirección de Epidemiología, Ministerio de Salud, Argentina) that dengue outbreaks seem to follow QB and QQ cycles over northern Argentina (region 8, in figures 2 and 5), and as such could be associated with natural variability of climate signals. This is particularly true for the Salta and Misiones provinces. Further and more comprehensive analyses are required since understanding sequences of the above events should help in predicting the re-emergence of such diseases.

The advanced knowledge of the phasings of climate signals (for high and low frequencies such as the QB and IA/QQ signals as identified in this paper) which are going to modulate local seasonal variability like the South American Monsoon System (SAMS, see figure 2 in Ma and Mechoso 2007) is a prerequisite to study and mitigate consequential impacts on public health. Working closely with entomologists and virologists to outline some mechanisms contributing to epidemics outbreaks also becomes a necessity. All relevant information (in near real-time) is to be distributed to stakeholders (including health officials) involved with health early warning systems (HEWS). Applied results should help in improving decision-making practices for best prevention and adaptation strategies of climate impact on human health and welfare (McMichael and Kovats 2000, Noireau *et al* 2005). The latter is very important in the climate change



context, modifying the so-called natural climate signals. In a forthcoming paper downscaled processes and mechanisms for epidemics outbreaks, possibly linked with climate–environment variability/change, will be assessed.

## Acknowledgments

YMT thanks Drs Mike Purdy and Arnold Gordon, Director of LDEO and Head of Physical Oceanography at LDEO, respectively, for unconditional support. Thanks are due to Andy Robertson from IRI for providing the PSA indices and to Pablo Orellano from the Health Ministry of Argentina. CHR thanks Silvia Quevedo for collaborating in the mapping of dengue fever distribution over South America. This work is part of the joint CNES-CONAE ‘MATE project’ on re-emerging epidemics in Argentina and which had been initiated by Dr Antonio Güell, Head of the Valorization–Application Department at CNES and Mr Felix Menicocci, General Secretary of CONAE. This is LDEO contribution # 7224.

## References

- Angell J K and Korshover J 1974 Quasi-biennial and long-term fluctuations in the centers of action *Mon. Weather Rev.* **102** 669–78
- Avilés G, Paz M V, Rangeon G, Ranaivoarisoa M Y, Verzari N, Roginski P and Enria D 2003 Laboratory surveillance of Dengue in Argentina, 1995–2001 *Emerg. Infect. Dis.* **9** 738–42
- Barbosa H A, Huete A R and Baethgen W E 2006 A 20-year study of NDVI variability over the Northeast region of Brazil *J. Arid Environ.* **87** 288–307
- Córdoba-Lanús E, De Grosso M L, Piñero J E, Valladares B and Salomón O D 2006 Natural infection of *Lutzomyia neivai* with *Leishmania* spp. in northwestern Argentina *Acta Trop.* **96** 1–5
- del Rosario Prieto M 2007 ENSO signals in South America: rains and floods in the Paraná river region during colonial times *Clim. Change* **83** 39–54
- Diaz L A *et al* 2006 Genotype III Saint Louis encephalitis virus outbreak, Argentina, 2005 *Emerg. Infect. Dis.* **12** 1752–4
- Diosque P *et al* 2004 Chagas diseases in rural areas of Chaco Province, Argentina: epidemiologic survey in humans, reservoirs, and vectors *Am. J. Trop. Med. Hyg.* **5** 590–3
- EID Updates 2008 Emerging and re-emerging infectious diseases, Region of the Americas, vol 5 <http://www.paho.org/English/AD/DPC/CD/eid-eer-2008-03-31.htm>
- ESSP 2004 Global environmental change and human health *Report No. 4: Science Plan and Implementation Strategy* ed U Confalonieri and A McMichael, p 79
- Fagundes A, Marzochi M, Fernandes O, Perez M A, Schubach A O, Schubach T, Amendoeira M, Mouta-Confort E and Marzochi K 2007 First encounter of sub-clinical human *Leishmania* (Viannia) infection in State of Rio Grande do Sul, Brazil *Mem. Inst. Oswaldo Cruz* **102** 8
- Garric G, Venegas C A, Tansley C E and James I N 2003 Atmosphere–sea–ice low-frequency variability with a simple model of the southern hemisphere *Q. J. R. Meteorol. Soc.* **129** 2347–66
- Gorla D E 2002 Variables ambientales registradas por sensores remotos como indicadores de la distribución geográfica de *Triatoma infestans* (Heteroptera: Reduviidae) *Ecol. Austral.* **12** 117–27
- Grimm A M, Ferraz S E T and Gomes J 1998 Precipitation anomalies in Southern Brazil associated with El Niño and La Niña events *J. Clim.* **11** 2863–80
- Guerra C A, Snow R W and Hay S I 2006 Defining the global spatial limits of malaria transmission in 2005 *Adv. Parasitol.* **62** 157–79
- Jarlan L, Tourre Y M, Mougín E, Philippon N and Mazzega P 2005 Dominant patterns of AVHRR NDVI interannual variability over the Sahel and linkages with key climate signals (1982–2003) *Geophys. Res. Lett.* **4** L04701
- Kaufmann R K, Zhou L, Knyazikhin Y, Shabanov N, Myneni R and Tucker C J 2000 Effect of orbital drift and sensor changes on the time series of AVHRR vegetation index data *IEEE Trans. Geosci. Remote Sens.* **38** 2584–97
- Kestin T S, Karoly D J, Yano J and Rayner N A 1998 Time Frequency variability of ENSO and stochastic simulations *J. Clim.* **11** 2258–72
- Lamberti R, Calvo C, Pombar A, Gino L, Alvarez E, Aguado C and Larrieu A 1999 Hydatidosis in the province of La Pampa, Argentina, 1998 *Bol. Chil. Parasitol.* **54** 110–2
- Los S O, Collatz G J, Bounoua L, Sellers P J and Tucker C J 2001 Global interannual variations in sea surface temperature and land surface vegetation air temperature and precipitation *J. Clim.* **14** 1535–49
- Lotsch A, Friedl M A, Anderson B T and Tucker C J 2003 Coupled vegetation–precipitation variability observed from satellite and climate record *Geophys. Res. Lett.* **30** 1774
- Ma H-Y and Mechoso C R 2007 Submonthly variability in the South American monsoon system *J. Met. Finish. Soc. Japan* **85** 385–401
- Mann M E and Park J 1994 Global scale modes of surface temperature variability on interannual to century timescales *J. Geophys. Res.* **99** 25819–933
- Mann M E and Park J 1996 Joint spatio-temporal modes of surface temperature and sea level pressure variability in the Northern Hemisphere during the last century *J. Clim.* **9** 2137–62
- Masson V, Champeaux J L, Chauvin F, Meriguet C and Lacaze R 2003 A global database of land surface parameters at 1 km resolution in meteorological and climate models *J. Clim.* **16** 1261–82
- McMichael A J and Kovats R S 2000 Climate change and climate variability *Environ. Monit. Assess.* **61** 49–64
- Minetti J L and Sierra E M 1989 The influence of general circulation patterns on humid and dry years in the cuyo andean region of Argentina *Int. J. Climatol.* **9** 55–68
- Mo K C 2000 Relationships between low-frequency variability in the Southern Hemisphere and sea surface temperature anomalies *J. Clim.* **13** 3599–620
- Mo K C and Paegle J N 2001 The Pacific–South American modes and their downstream effects *Int. J. Climatol.* **21** 1211–29
- Myneni R B, Los S L and Tucker C J 1996 Satellite based identification of linked vegetation index and sea surface temperature anomaly areas from 1982 to 1990 for Africa, Australia and South America *Geophys. Res. Lett.* **23** 729–32
- Noireau F, Rojas Corteza M G, Monteiro F A, Jansene A M and Torrico F 2005 Can wild *Triatoma infestans* foci in Bolivia jeopardize Chagas disease control efforts? *Trends Parasitol.* **21** 7–10
- North G R, Bell T L, Cahalan R F and Moenig F J 1982 Sampling errors in the estimation of empirical orthogonal functions *Mon. Weather Rev.* **110** 669–706
- Paruelo J M, Garbulski M F, Guerschman J P and Jobbagy E G 2004 Two decades of normalized difference vegetation index changes in South America: identifying the imprint of global change *Int. J. Remote Sens.* **25** 2793–806
- Patz J A *et al* 2004 Unhealthy landscapes: policy recommendations on land use change and infectious disease emergence. Working group on land use change and disease emergence *Environ. Health Perspect.* **10** 1092–8

- Pisciottano G, Diaz A D, Cazes G and Mechoso C R 1994 El Niño-Southern Oscillation impact on rainfall in Uruguay *J. Clim.* **7** 1286–302
- Podesta G P, Messina C D, Grondona M O and Magrin G O 1999 Associations between grain crop yields in central eastern Argentina and El Niño southern oscillation *J. Appl. Meteorol.* **38** 1488–98
- Polop F, Provencal C, Scavuzzo M, Lamfri M, Calderón G and Polop J 2008 On the relationship between the environmental history and the epidemiological situation of Argentine hemorrhagic fever *Ecol. Res.* **23** 217–25
- Porcasi X, Calderón G E, Lamfri M, Scavuzzo M, Sabattini M S and Polop J J 2005 Predictive distribution maps of rodent reservoir species of zoonoses in Southern America *Mastozool. Neotrop.* **12** 199–216
- Poveda G, Roja W, Quinones M L, Velez I D, Mantilla R I, Ruiz D, Zuluaga J S and Rua G L 2001 Coupling between annual and ENSO timescales in the malaria-climate association in Colombia *Environ. Health Perspect.* **109** 489–93
- Ribera P and Mann M E 2003 ENSO related variability in the southern hemisphere (1948–2000) *Geophys. Res. Lett.* **30** 1006
- Richman M B 1986 Rotation of principal components *J. Climatol.* **6** 293–335
- Robertson A W and Mechoso C R 2003 Circulation regimes and low-frequency oscillation in the south Pacific sector *Mon. Weather Rev.* **131** 1566–76
- Root T L, Price J T, Hall K R, Schneider S H, Rosenzweig C and Pounds J A 2003 Fingerprints of global warming on wild animals and plants *Nature* **421** 57–60
- Ropelewski C E and Halpert M S 1987 Global and regional scale of precipitation and temperature patterns associated with the El Niño/southern oscillation *Mon. Weather Rev.* **115** 1606–26
- Sergio Sosa-Estani S, Salomón O D, Gómez A O, Esquivel M L and Segura E L 2001 Regional differences and Hantavirus pulmonary syndrome (an emerging and tropical disease in Argentine) *Cad. Saúde Pública* **17** 47–57
- Servain J 1991 Simple climatic indices for the tropical Atlantic Ocean and some applications *J. Geophys. Res.* **96** 15137–46
- Slayback D A, Pinzon J E, Los S O and Tucker C 2003 Northern hemisphere photosynthetic trends 1982–1999 *Global Change Biol.* **9** 1–15
- Tourre Y M, Rajagopalan B and Kushnir Y 1999 Dominant patterns of climate variability in the Atlantic Ocean during the last 136 years *J. Clim.* **12** 2285–99
- Tourre Y M and White W B 2005 Evolution of the ENSO signal over the tropical Pacific–Atlantic domain *Geophys. Res. Lett.* **32** L07605
- Tourre Y M and White W B 2006 Global climate signals and equatorial SST variability in the Indian, Pacific and Atlantic oceans during the 20th century *Geophys. Res. Lett.* **33** L06716
- Trenberth K E and Shin W T K 1984 Quasi-biennial fluctuations in sea level pressures over the northern hemisphere *Mon. Weather Rev.* **112** 761–77
- Trewavas A 2002 Malthus foiled again and again *Nature* **668–70**
- Tseng L and Mechoso C R 2001 A quasi-biennial oscillation in the equatorial Atlantic Ocean *Geophys. Res. Lett.* **28** 187–90
- Tucker C J 1979 Red and photographic infrared linear combinations for monitoring vegetation *Remote Sens. Environ.* **8** 127–50
- Tucker C J, Pinzon J E, Brown M E, Slayback D, Pak E W, Mahoney R, Vermote E and El Saleous N 2005 An extended AVHRR 8-km NDVI Data Set Compatible with MODIS and SPOT VEGETATION data *Int. J. Remote Sens.* **26** 4485–98
- Van den Hurk B, Viterbo J J M and Los S O 2003 Impact of leaf area index seasonality on the annual land surface evaporation in a global circulation model *J. Geophys. Res.* **108** 4191
- Venegas S A, Mysak L A and Straub D N 1996 Evidence for interannual and interdecadal climate variability in the South Atlantic *Geophys. Res. Lett.* **23** 2673–6
- Weisberg R H and Wang C 1997 Slow variability in the equatorial west-central Pacific in relation to ENSO *J. Clim.* **10** 1998–2017
- White W B 2004 Comments on synchronous variability in the southern hemisphere atmosphere, sea ice and ocean resulting from the annular mode *J. Clim.* **17** 2249–54
- White W B and Allan R J 2001 A global quasi-biennial wave in surface temperature and pressure and its decadal modulation from 1900 to 1994 *J. Geophys. Res.* **106** 26789–803
- White W B and Petersen R 1996 An Antarctic circumpolar wave in surface pressure, wind, temperature, and sea ice extent *Nature* **380** 699–702
- Yates T L *et al* 2002 The ecology and evolutionary history of an emergent disease: hantavirus pulmonary syndrome *Bioscience* **52** 989–98